
Evaluation of a Rate-Dependent, Elasto-Plastic Cohesive Zone Mixed-Mode Constitutive Model for Spot Weld Modeling

Matthias Bier¹, Christian Liebold¹, André Haufe¹, Herbert Klamser²

¹DYNAmore GmbH, Stuttgart, Germany

²Dr. Ing. h.c. F. Porsche AG, Weissach, Germany

Abstract:

Currently, there are several material models implemented in LS-DYNA which are more or less capable to simulate a spot weld behavior under crash conditions. The material parameters for crash simulations are determined by comparing the results of tensile, shear and peel tests specimen with an equivalent FE-model. By varying the spot weld material parameters, the simulation should reproduce the test and its results as accurate as possible. Important parameters that should be reproduced by the simulation are the displacement and the force at which the spot weld fails. With finely discretized models that divide the spot weld into several heat affected zones to consider as many deformation and failure phenomena as possible, the tests and their results can be rebuild quite precisely. The main disadvantage of these detailed models is that they require the use of approximately 50.000 solid elements for the spot weld only. This leads for explicit time integration schemes to very small time steps and therefore to computation times that are far too high for crash simulations.

For this reason less detailed (i.e. coarse) models are needed to describe the behavior of spot welds during crashworthiness simulations. Spot welds are herein modeled with beam or solid elements that connect the two coarsely meshed flange partners modeled by shell elements. Usually *MAT_SPOTWELD_DAIMLERCHRYSLER (*MAT_100_DA) is used to describe the spot weld's constitutive behavior. Using *MAT_100_DA, the parameters that define the onset of failure can be the effective plastic strain or a criteria incorporating a combination of axial, shear and bending stresses.

Since spot welds in automotive structures not only show rate-dependent, elasto-plastic material behavior but also exhibit different stiffness properties in uniaxial and shear loading, the so called *MAT_COHESIVE_MIXED_MODE_ELASTOPLASTIC_RATE (*MAT_240) material card offers new possibilities to define the point of failure by using the energy release rates G_{Ic} and G_{IIc} and the yield stresses in mode I and II fracture as failure criterion independently. Additionally, the rate-dependency in deformations can be considered using either a linear logarithmic or quadratic logarithmic model.

In the present paper, the material behavior of a spot weld modeled with one solid element using *MAT_100 and a spot weld modeled with one, four or eight solid elements using *MAT_240 are compared with the results of a very detailed simulation describing the spot weld's behavior during tensile, shear and peel test. To predict the spot weld's behavior under various geometrical conditions, its alignment with regard to the flange mesh has been modified in steps of 30°, 45° and 60° from its original central position. Finally, an adaptive mesh is used for the flanges that are bonded by the spot weld to analyze the mesh size influence on the spot weld's failure behavior.

Keywords:

spot weld, cohesive zone model, rate-dependency, elasto-plastic material behavior, failure, adaptive mesh

1 Introduction

Today's crash simulation models are getting more and more detailed, due to the fact that correct failure prediction techniques either for parts or for connection details are necessary to successfully design bodies in white prior to the hardware test. Therefore, it is necessary to model the behavior of the connection details like spot welds as exact as possible in order to avoid inaccuracies that influence the predictiveness of the whole model. Today roughly 4 to 6 thousand spot welds are used in a detailed car crash simulation where sheet metal is combined with different material types and thicknesses. It is important to understand the behavior of spot welds under various load combinations and to develop models which are able to simulate their behavior as accurate as possible in the context of a reasonable amount of computation time. Considering heat affected zones and using more than 50.000 solid elements, it is clearly possible to simulate the spot weld behavior in tensile, shear and peel tests with a KSII specimen very precisely. Since these models require extremely long computation times, they are not suitable for full car crash analysis and other, rather simplified spot weld models have to be used instead. Therefore, LS-DYNA already offers many different modeling possibilities that are regularly reworked and enhanced by new concepts and ideas.

In the following, the results of a coarse spot weld model which uses *MAT_240 (*MAT_COHESIVE_MIXED_MODE_ELASTOPLASTIC_RATE) as spot weld constitutive model connecting two DC04 steel plates are presented. The spot weld is simulated with one, four or eight solid elements. The spot weld's behavior during a tensile, shear and peel test are computed and compared to the results of a very accurate and detailed model that is basically build out of solid elements using *MAT_120 (*MAT_GURSON) to simulate the sheet metals, the spot weld and the heat affected zones [5]. The results are compared with another coarse model that uses *MAT_100_DA (*MAT_SPOTWELD_DAIMLERCHRYSLER) as spot weld constitutive model but comprises only one solid element for the spot weld. To have a better understanding of the spot weld's behavior during several simulation conditions its orientation has been changed towards the flange mesh in steps of 30°, 45° and 60°. In addition its position with respect to the mesh has been varied by moving the mesh 1.5 mm in x-, z- or x- or z-direction. Furthermore the effect of an adaptively generated mesh has been investigated and the spot weld was directly connected to the shell elements of the flange sheets. Furthermore by splitting 16 shell elements that surround the spot weld into four elements each, i.e. refining the flange, the failure behavior of the spot weld has been studied in detail.

To get an impression how the surrounding flange discretization influences the spot weld's failure behavior, DC04 material parameters have been substituted in the vicinity of the spot weld with stiffer material parameters of DP600 sheet metal. Here 16 shell elements surrounding the spot weld where modeled with the DP600 parameters while the sport weld was directly meshed to the flange mesh.

2 Models and Variations

The models were supposed to simulate a KS II specimen during a tensile, shear and peel test. KS II specimen that are also called tensile-shear-specimen are quite common samples to test all different kinds of joints under laboratory conditions [2]. A combination of both, tensile and shear test is possible with this specimen but this case was not taken into account in the present investigation.

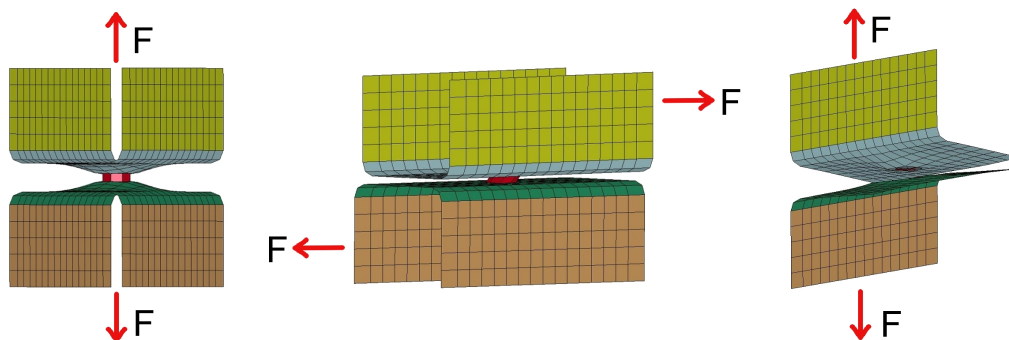


Figure 1: Coarse KS II models during tensile (left), shearing (middle) and peeling test (right)

The main parameters that were to be reproduced with the coarse model were the force and the displacement at which the spot weld fails. The material parameters of *MAT_240 were adapted for the tensile and shear test in a way such that the results of the detailed model were resembled as close as

possible. With these parameters, the peeling test and the models with different spot weld positions and orientations were simulated. The coarse model using the *MAT_100_DA had already calibrated material parameters and was used as an additional reference.

2.1 Coarse spot weld models

The figure above (Fig. 1) already shows the coarse models that were used for the computations. Two DC04 sheet metals are simulated with shell elements having a thickness of 1.5 mm at each integration point by using the “Belytschko-Tsay” element formulation. The material model that was used to simulate the connected sheet metals was *MAT_GURSON. The vertical parts of the sheet metal were also modeled with shell elements but *MAT_RIGID was used herein. As mentioned before, the spot weld is modeled with one, four or eight solid elements and *MAT_240. An additional coarse model which was modeled in the same way, used *MAT_100_DA and only one solid element for the spot weld.

The elastic response of the testing machine performing the tests was simulated as a spring applying the movement of the machine to the upper specimen. For the tensile test, the lower vertical sheet metals are bound to their original position with a simulated spring. The movement of these sheets during the shear and peel test is totally restricted with boundary conditions.

2.2 Variations of the coarse spot weld model

To compare the spot weld's behavior under several conditions, the position with respect to the flange mesh was modified by rotating the spot weld around its z-axis in steps of 30°, 45° and 60° compared to its original position (Fig. 2).

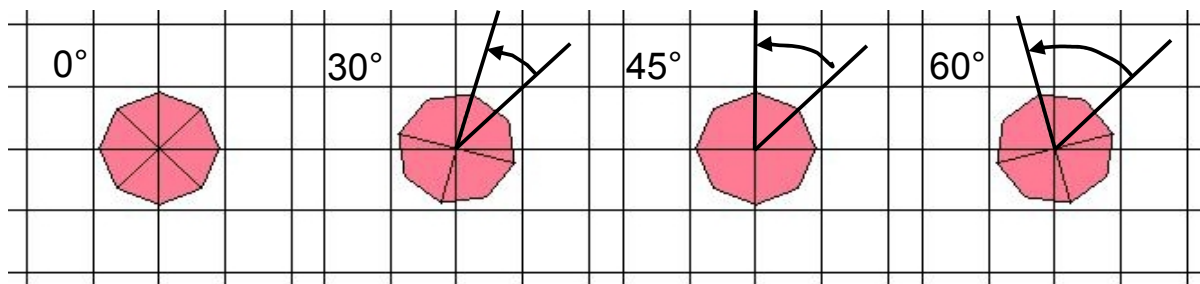


Fig. 2: Spot weld after rotation - on the left, the spot weld is in its original position

Moving the mesh in steps of 1.5 mm in x-, z- and both, x- and z-direction (Fig. 3), allowed to study the effect of how the results of the simulation depend on the position of the spot weld's center. It is either located on the edge or in the center of a shell element.

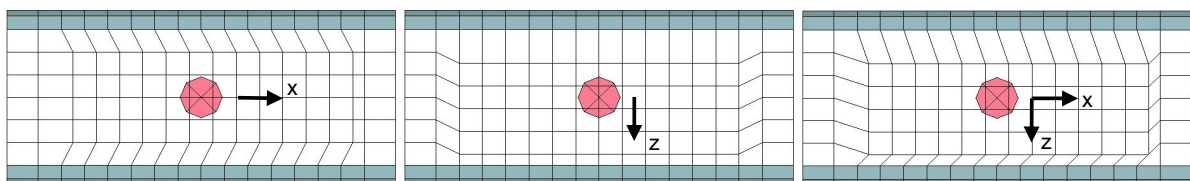


Fig. 3: Spot weld position according to the mesh – mesh moved in steps of 1.5 mm into x- (left), z- (middle) and x-z-direction (right)

As a third variation the mesh around the spot weld was modified. In a first approach, 16 shell elements surrounding the spot weld were split into four elements each. In a second step, the nodes of the spot weld were directly meshed to the flange mesh where eight elements build an octagon around the spot weld (in case it is build out of four solid elements), another twelve elements will then connect these elements to the regular mesh (Fig. 4). In the latter case the use of contact definitions between the spot weld and sheet metals is unnecessary.

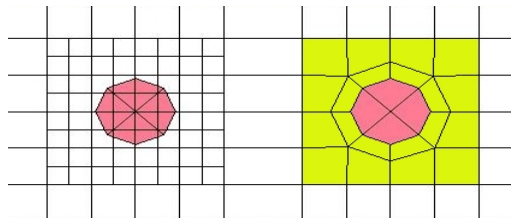


Fig. 4: Fine mesh around the spot weld (left) and direct connection with the shell elements (right)

2.3 Detailed spot weld model

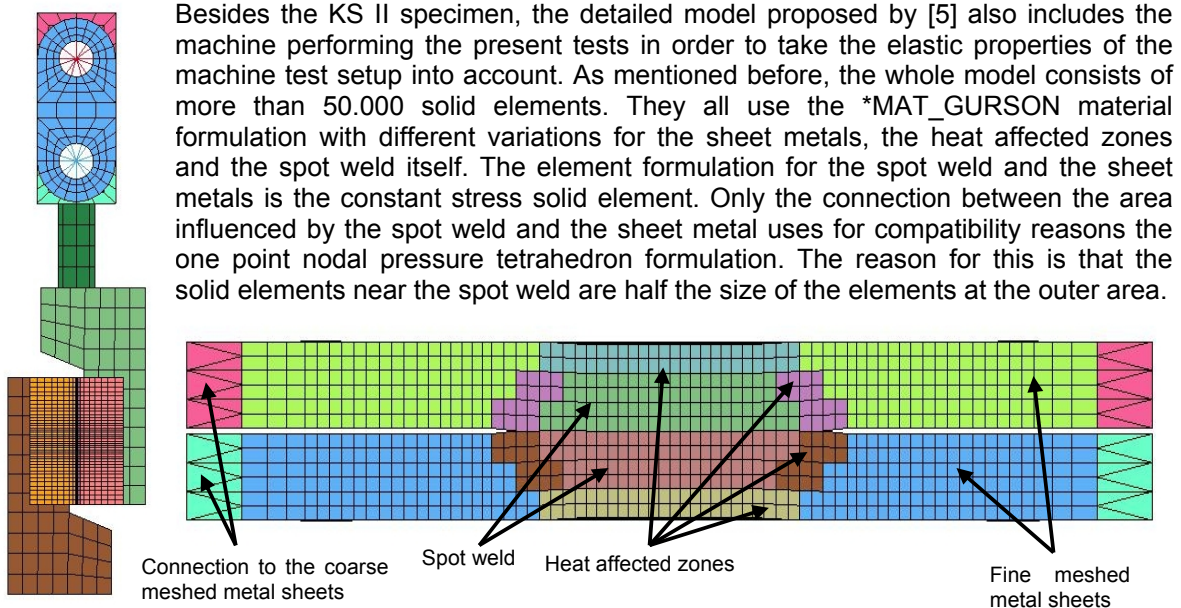


Fig. 5: KS II specimen inside the testing machine (left). Highly detailed spot weld model with its several heat affected zones and the connection to the regular metal sheets (right) proposed by [5]

3 Material models

Since most of the material models used for the present computations are quite known, only *MAT_240 will be presented in more detail with the restriction that only parameters are discussed that were used in this study. For further information on the other constitutive models, please refer to the LS-DYNA manual [1].

3.1 MAT_COHESIVE_MIXED_MODE_ELASTOPLASTIC_RATE (*MAT_240)

The *MAT_240 material card considers both the effects of rate-dependency and plasticity with a tri-linear traction-separation law that reminds one of the *MAT_185 constitutive model. It is a tri-linear elastic-ideally plastic cohesive zone model. The separation at the point of failure is plastic [3] such that no brittle fracture behavior can be modeled with this type of material. The mixed-mode separation is determined by combining the separation in normal and tangential direction as follows:

$$\Delta_m = \sqrt{\Delta_n^2 + \Delta_t^2} \quad (1)$$

whereas the separation in normal direction Δ_n and in tangential direction Δ_t are computed from the element's separation in the integration points:

$$\Delta_n = \langle u_n \rangle \quad \text{and} \quad \Delta_t = \sqrt{u_{t1}^2 + u_{t2}^2}, \quad \langle x \rangle = \begin{cases} x & \text{if } x > 0 \\ 0 & \text{else} \end{cases} \quad (2)$$

u_n , u_{t1} and u_{t2} are the separations in the normal and the two tangential directions of the element's coordinate system.

Since a parameter for the element's cohesive thickness was chosen to be bigger than zero, the initial stiffness for both modes is computed based on the user defined Young's and shear modulus.

$$E_n = \frac{EMODUL}{THICK} \quad \text{and} \quad E_t = \frac{GMODUL}{THICK} \quad (3)$$

Another parameter which describes the shape of the traction-separation law has to fulfill the following requirements:

$$0 \leq f_{G1} = \frac{G_{I,P}}{G_{IC}} < 1 - \frac{T^2}{2G_{IC}E_n} < 1 \quad \text{for mode I loading,} \quad (4)$$

$$0 \leq f_{G2} = \frac{G_{II,P}}{G_{IIC}} < 1 - \frac{S^2}{2G_{IIC}E_t} < 1 \quad \text{for mode II loading.} \quad (5)$$

f_{G1} and f_{G2} are always constant parameters. For the spot weld simulation values for S, T, G_{IC} and G_{IIC} were chosen to be greater than zero. Therefore, the yield stresses in mode I and II (T and S) are not a function of the equivalent strain rate but have a constant value:

$$T(\dot{\epsilon}_{ep}) = T0 \quad \text{and} \quad S(\dot{\epsilon}_{ep}) = S0. \quad (6)$$

The energy release rates in both modes G_{IC} and G_{IIC} are therefore also constant values specified by the user and show no rate-dependency.

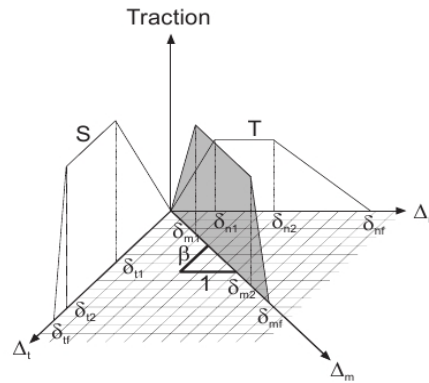


Fig. 6: Tri-linear, mixed mode traction-separation law

With these parameters describing the single modes, the mixed-mode material behavior was computed using a quadratic approach for the yield stress and a damage initiation criterion. The damage evolution follows the power law. The mixed-mode yield initiation displacement is defined as:

$$\delta_{m1} = \delta_{n1} \delta_{t1} \sqrt{\frac{1 + \beta^2}{\delta_{t1}^2 + (\beta \delta_{n1})^2}} \quad (7)$$

with $\delta_{n1} = T/E_n$ and $\delta_{t1} = S/E_t$ for the single-mode yield initiation displacements and $\beta = \delta_{t1} / \delta_{n1}$ for the mixed-mode ratio. The damage initiation displacement is defined in a similar way:

$$\delta_{m2} = \delta_{n2} \delta_{t2} \sqrt{\frac{1 + \beta^2}{\delta_{t2}^2 + (\beta \delta_{n2})^2}} \quad (8)$$

with $\delta_{n2} = \delta_{n1} + f_{G1} G_{IC} / T$ in normal- and $\delta_{t2} = \delta_{t1} + f_{G2} G_{IIC} / S$ in tangential-direction.

The final failure displacement can furthermore be computed as the power law damage evolution:

$$\delta_{mf} = \frac{\delta_{m1} (\delta_{m1} - \delta_{m2}) E_n G_{IIC} \cos^2 \gamma + G_{IC} (2G_{IIC} + \delta_{m1} (\delta_{m1} - \delta_{m2}) E_t \sin^2 \gamma)}{\delta_{m1} (E_n G_{IIC} \cos^2 \gamma + E_t G_{IC} \sin^2 \gamma)} \quad (9)$$

$$\text{with } \gamma = \arccos\left(\frac{\langle u_n \rangle}{\delta_m}\right). \quad (10)$$

The plastic separation in each element direction is subsequently computed. The separation in peel direction is given by:

$$u_{n,P} = \max(u_{n,P,\Delta t-1}, u_n - \delta_{m1} \sin \gamma, 0). \quad (11)$$

In shear direction, a shear yield separation is defined as:

$$\delta_{t,y} = \sqrt{(u_{t1}^2 - U_{t1,P,\Delta t-1})^2 + (u_{t2}^2 - U_{t2,P,\Delta t-1})^2}. \quad (12)$$

The plastic shear separations in the element coordinate system will be updated, when $\delta_{t,y} > \delta_{m1} \sin \gamma$:

$$\begin{aligned} u_{t1,P} &= u_{t1,P,\Delta t-1} + u_{t1} - u_{t1,\Delta t-1} \\ u_{t2,P} &= u_{t2,P,\Delta t-1} + u_{t2} - u_{t2,\Delta t-1} \end{aligned} \quad (13)$$

Once Δ_m reaches δ_{m2} , the damage initiation criterion is satisfied and the damage variable D increases:

$$D = \max\left(\frac{\Delta_m - \delta_{m2}}{\delta_{mf} - \delta_{m2}}, D_{\Delta t-1}, 0\right). \quad (14)$$

The element fails in the corresponding integration point if Δ_m is greater than δ_{mf} , respectively D is equal to one.

3.2 MAT_100_DAIMLERCHRYSLER (*MAT_100_DA)

The *MAT_100_DA material model is the standard spot weld model implemented in LS-DYNA. With option OPT=8 it shows a bi-linear, elasto-plastic material behavior [2] enhanced by a state-of-the-art failure concept.

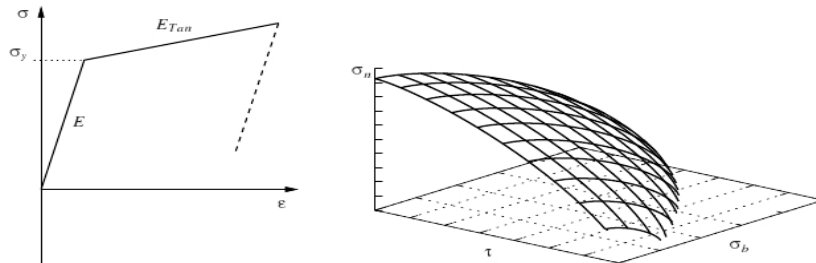


Fig. 7: Material (left) and failure (right) model for *MAT_SPOTWELD_DA

In contrast to *MAT_240, a stress based failure criterion is taken into account. The damage type which is used for the *MAT_100_DA material is DG_TYPE = 4 which considers a fading energy based damage [1]. The failure parameters for normal stress (S_n), bending stress (S_b) and shear stress (S_s) are considered via the *DEFINE_CONNECTION_PROPERTIES card. Therefore, the failure criterion is defined as:

$$f = \left(\frac{\sigma_n}{S_n}\right)^{m_n} + \left(\frac{\sigma_b}{S_b}\right)^{m_b} + \left(\frac{\tau}{S_s}\right)^{m_s} - 1. \quad (15)$$

Damage will be initiated, once $f \geq 0$ and will occur, when the damage growth ω which is a function of the plastic strain is greater than 1. Damage type 4 considers the internal work done by the spot weld after its failure and is supposed to be more realistic than other damage types.

3.3 MAT_GRUSON (*MAT_240)

The *MAT_GURSON material model is a dilatational-plastic model which is available for both, shell and solid elements [1]. Since the LS-DYNA release 971, strain-rate dependency can be applied as well. This model considers the nucleation, coalescence and growth of voids within the Gurson yield function:

$$\Phi = \frac{\sigma_M^2}{\sigma_Y^2} + 2q_1 f^* \cosh\left(\frac{3q_2 \sigma_H}{2\sigma_Y}\right) - 1 - (q_1 f^*)^2 = 0. \quad (16)$$

σ_M is the equivalent von Mises stress, σ_Y the yield stress and σ_H the mean hydrostatic stress. An effective void volume fraction function $f^*(f)$ is defined that considers the critical void volume fraction (point at which voids begin to aggregate) and the failure void volume fraction. An additional function which describes the growth of the void volume fraction takes the growth of existing voids and the nucleation of new voids during tension into account.

4 Comparison of the material models for spot weld simulations

In a first step, the *MAT_240 constitutive parameters were adapted in a way that the main criteria that were gained from the failure of the detailed spot weld model were fulfilled: force and displacement at which the spot weld fails. If this was not possible, the results of the *MAT_100_DA material model were tried to be reproduced. The material parameters are adapted for the tensile and shear test with a spot weld model using four solid elements and the *MAT_240 material card. All other computations were subsequently performed with these constitutive parameters such that the results of the peeling test were also an indicator for the quality of the model. In the following all diagrams are depicted in force vs. time units for simplicity reasons, since due to a constant loading velocity this correlates directly to the measured displacements.

4.1 Results of the tensile, shearing and peeling test

First, the results of the adapted material parameters for the tensile and shear test together with the result that were obtained for the peel test are presented in Fig. 8.

The results show that one is able to adapt the constitutive parameters for *MAT_240 in such a way that at least the same point of failure as for the model using the *MAT_100_DA in combination with one solid element during the tensile test can be gained. For the shear test, even better results are obtained, whereupon the results of the peel test are not as good as the results for the *MAT_100_DA material model. A saltus in the force-time curve usually indicates the failure of at least one of the solid elements and is especially visible at the curves with eight solid elements for the spot weld.

Based on these results, the material parameters for the computations with one and eight solid elements were not adapted since it was not expected to deliver better results than with four solid elements. An indicator for this was the fact that the curve's slope at the beginning of the computation was approximately the same in all the three cases. As shown in (4.4), the gradient of the curve at the beginning of the computation is highly dependent on the material grade surrounding the spot weld and therefore, adapting the material parameters for one or eight solid elements would probably just lead to similar results as with four solid elements.

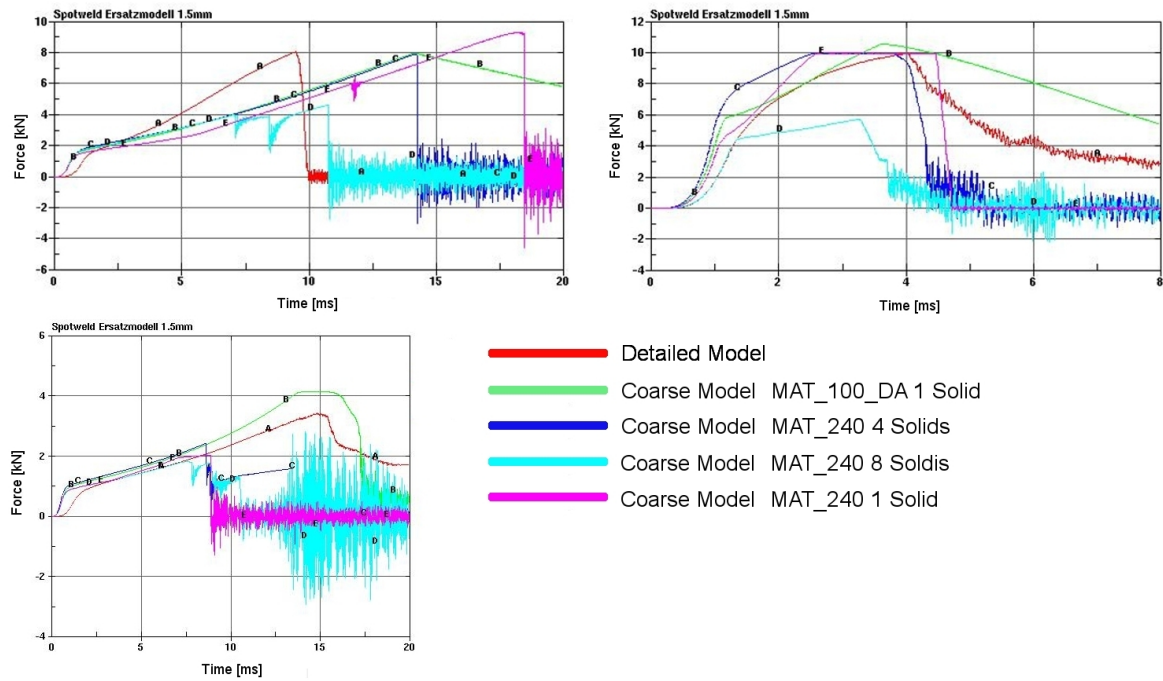


Fig. 8: Results for the tensile (upper-left), shearing (upper-right) and peeling test (lower-left).

4.2 Variations of the spot weld position

In the following the results that were obtained when the spot weld was rotated or its position was modified in relation to the flange mesh are presented. The curves for the detailed model are the same as the ones shown above (Fig. 8) since no variations are performed here – the spot weld's position was only changed in the coarse models. The constitutive parameters were carried over from the tensile and shear test of the first approach that reproduce the behavior of the detailed model.

4.2.1 Influence of the spot weld's rotation

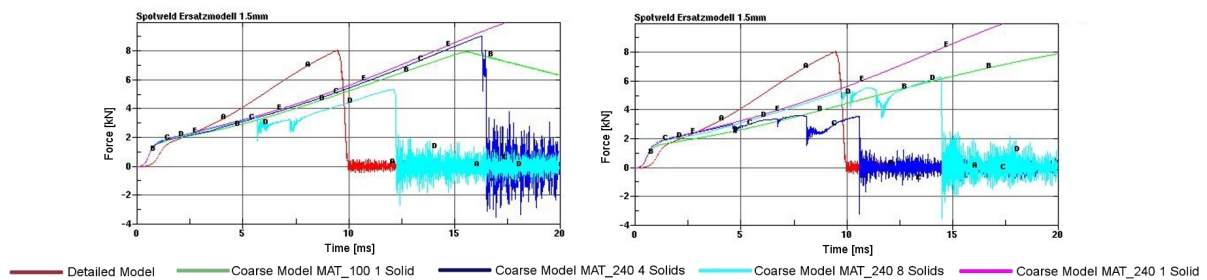


Fig. 9: Tensile test simulation results with spot welds rotated in steps of 30°(left), 45° (right)

The curves for a rotation of 30° and 60° show almost the same results for the tensile test simulation and therefore, only the results for a rotation of 30° and 45° of the spot weld are shown above (Fig. 9). The computations with four and eight solid elements applying *MAT_240 and the computation with one solid element applying *MAT_100_DA seem to be quite stable. For geometrical reasons, it is obvious that a rotation of 45° leads to the biggest influence on the results. In that case, both spot weld models using only one solid element did not fail at the expected displacement. The only combination that does not fail in all the three cases is the one using one solid element in combination with *MAT_240.

All models using one, four or eight solid elements in combination with *MAT_240 or one solid element in combination with *MAT_100_DA seem to be insensitive against rotation of the spot weld during the shearing test simulation. The curves show approximately the same results compared to the curves obtained from the regular shear test simulation. Except the curve for one solid element with *MAT_240 appears to be steeper in the beginning compared to the results of the regular computation.

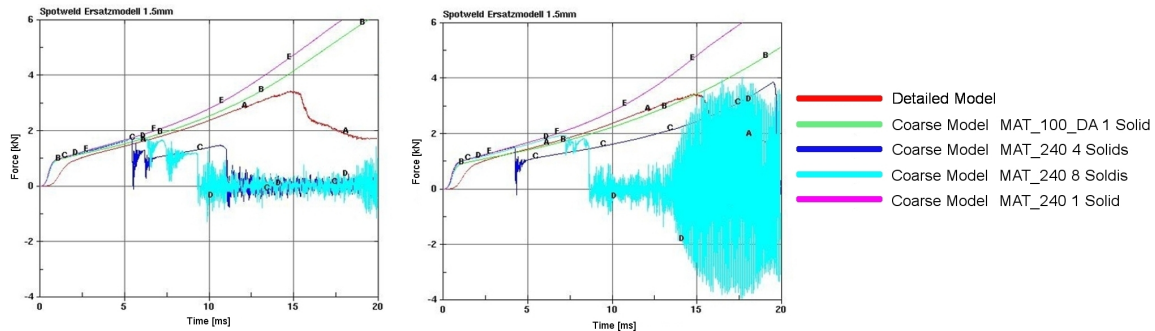


Fig. 10: Peeling test simulation results with spot welds rotated in steps of 30°(left), 45° (right).

Both models containing *MAT_100_DA and *MAT_240 do not lead to satisfactory results in the peel test (Fig. 10). It is remarkable that the models with four and eight solid elements using *MAT_240 do at least fail during the considered deformation. The simulations using only one solid element do not show any spot weld failure. Like the tensile test simulations, the results of a rotation of 30° and 60° are almost the same and therefore, the diagram for the 60° spot weld rotation is not shown here.

4.2.2 Influence of the spot weld's position related to the mesh

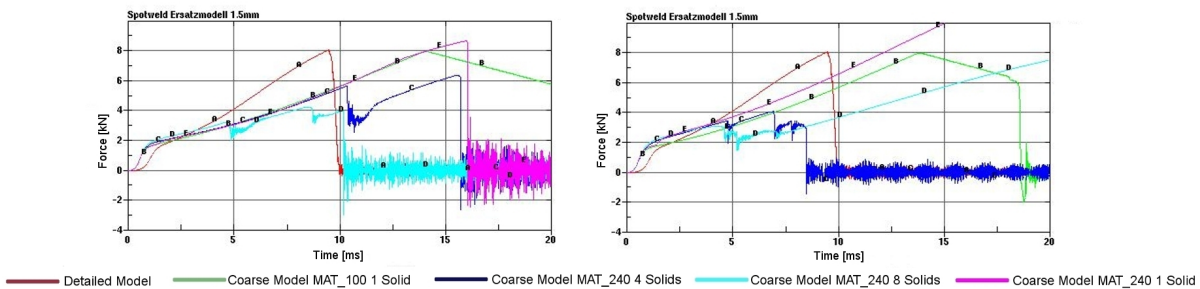


Fig. 11: Tensile test simulation results with the mesh moved in steps of 1.5 mm in x-(left) and x-z-direction (right).

A displacement of the mesh in x-direction almost has no influence on the point of the spot weld's failure during the tensile test compared to the mesh's displacement into z-direction. In that case, models using one and eight solid elements combined with *MAT_240 do not fail at all. The curves look similar to the ones that are shown in the diagram for the displacement in x-z-direction (Fig.11). Using one solid element in combination with *MAT_100_DA seems to be stable with respect to the movement of the mesh in all the three test cases.

Like the computations with the rotated spot welds, the curves for the shear test simulation with a modified mesh are similar to the ones that were obtained with the regular shear test calculation (Fig. 8).

In the peel test simulation, especially models using *MAT_240, a high dependency on the spot weld position related to the flange mesh is observed. While the spot welds fail too early in case the mesh is moved into x-direction, the model with one solid using *MAT_240 does not fail at all when the mesh is moved into z-direction or into x-z-direction. The diagrams below only show the results for the x- and the x-z-displacement of the mesh since the movement into z-direction seems to have the biggest influence on the spot weld's failure behavior. Like the tensile test simulation, the model with one solid element in combination with *MAT_100_DA seems to be the most stable one.

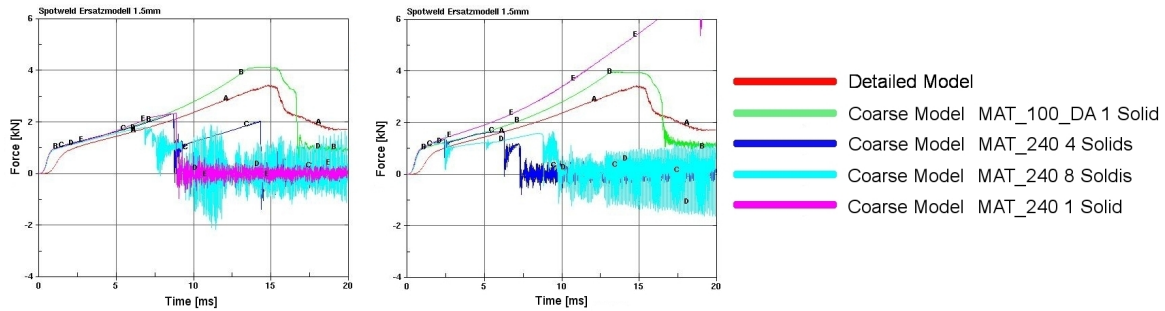


Fig. 12: Peeling test simulation results with the mesh moved in steps of 1.5 mm in x-(left) and x-z-direction (right).

4.3 Variations of the mesh

This section will show the results of the computations using either a halved mesh length around the spot weld or a direct connection between the spot weld and the mesh as shown above (Fig. 4). In a third section, the results of a spot weld simulation with an adaptive mesh for the sheet metals are shown. The material parameters that were used for the computations are identical to the investigations above.

4.3.1 Half mesh size around the spot weld

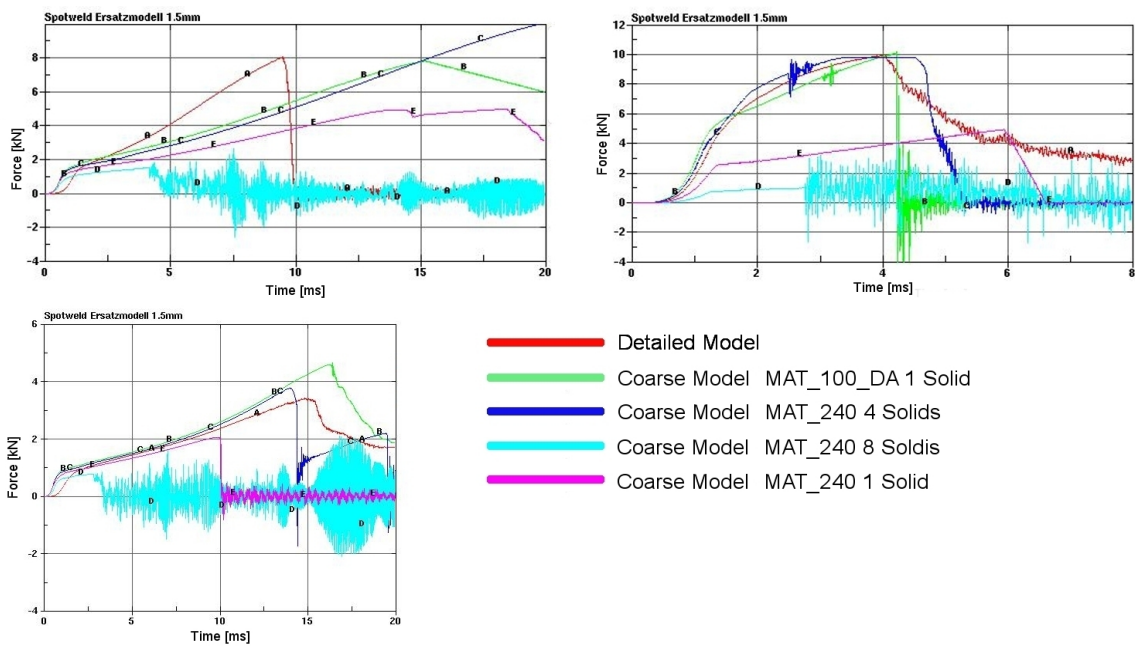


Fig. 13: Tensile (upper-left), shearing (upper-right) and peeling (lower-left) test simulation results with halved mesh length around the spot weld

With half the mesh size in the area surrounding the spot weld but unaltered material parameters, the models with *MAT_100_DA show the most stable results. The *MAT_240 model with four solid elements shows the best results of all three models using the *MAT_240 constitutive model but usually the spot welds fail later than the ones from the reference models. During the tensile test simulation, the coarse model with four solids for the spot weld using *MAT_240 does not fail at all.

4.3.2 Direct connection between the spot weld and the mesh

A direct connection between the spot weld and the mesh does not show any significant new results: the results seem to be quite good for all model variations during the shearing test simulation. In the tensile test simulation, models using *MAT_240 as spot weld material do not fail at all. The peeling test simulation shows that all models fail almost at the same time, except for the model using *MAT_100_DA. It seems that a direct connection between the spot weld and its surrounding material might be a better option for a peeling test when *MAT_240 is used as spot weld material, but clearly this will be only the second choice for every day engineering practice.

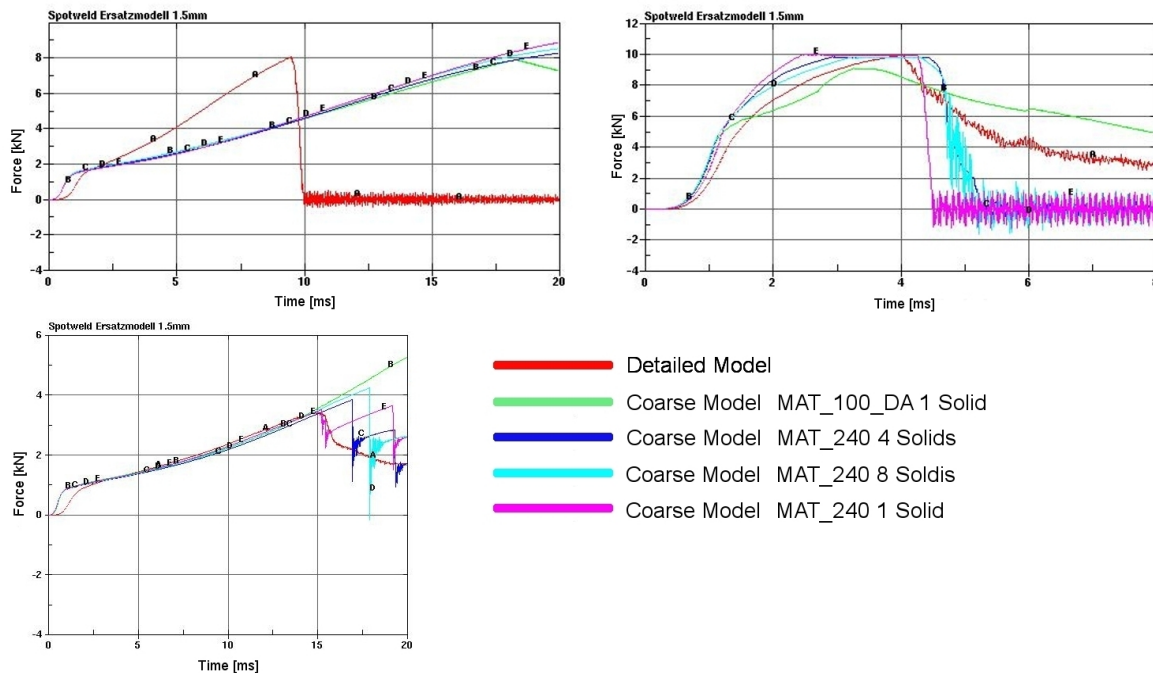


Fig. 14: Tensile (upper-left), shearing (upper-right) and peeling (lower-left) test simulation results with a direct connection between the spot weld and the mesh

4.3.3 Adaptive mesh

An adapted mesh on the two flange sheets was used to see which influence this might have on the spot weld's point of failure. The constitutive parameters of the *MAT_240 card are now adapted for the tensile and shearing test simulation with four solid elements simulating the spot weld. These results are subsequently used with four solid elements for the peeling test simulation and for all the other computations with one and eight solid elements.

The adaptivity of the mesh is activated in LS-DYNA by setting the ADPOPT in the corresponding *PART card to one. This activates the H-adaptivity for 3-D shell elements [4]. Adaptivity is then controlled by the *CONTROL_ADAPTIVE card. As adaptive option the angle change in degrees of one element compared to its surrounding elements was chosen. In the present case, the adaptive tolerance is set to five degrees which means that the mesh will be refined if the element shows an angle change of five degrees in comparison to its surrounding elements. The frequency for the adaptive refinement is set to five milliseconds hence during one computation, the mesh is refined up to four times since the angle change between the elements is checked every five milliseconds simulation time up to 20 milliseconds. In the adaptivity control card, the ADPASS option is set to one hence every time the mesh is refined the program continues to calculate directly with the refined mesh.

The results below show that it is possible to adapt the *MAT_240 parameters of the coarse model in such a way that at least the results of the shear test can be reproduced (Fig. 16). For the tensile test, it is not possible to get close to the results of the *MAT_100_DA model since introduction of a finer mesh in the surrounding of the spot weld leads to a kinematical more flexible discretization: The failure occurs at roughly the same displacement but at lower force. Since the results of the model using only one solid element and *MAT_240 for the spot weld are quite good for the peel test, it might be worth a try to combine simple spot weld models with an adapted mesh.

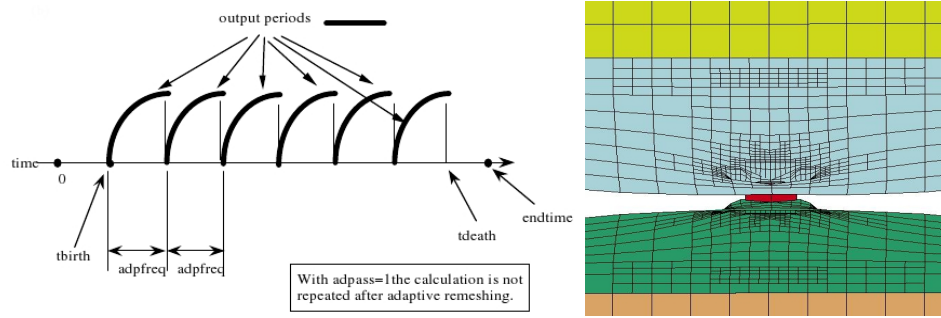


Fig. 15: Illustration for ADPASS = 1 (left) and spot weld with adaptive mesh during peeling test (right)

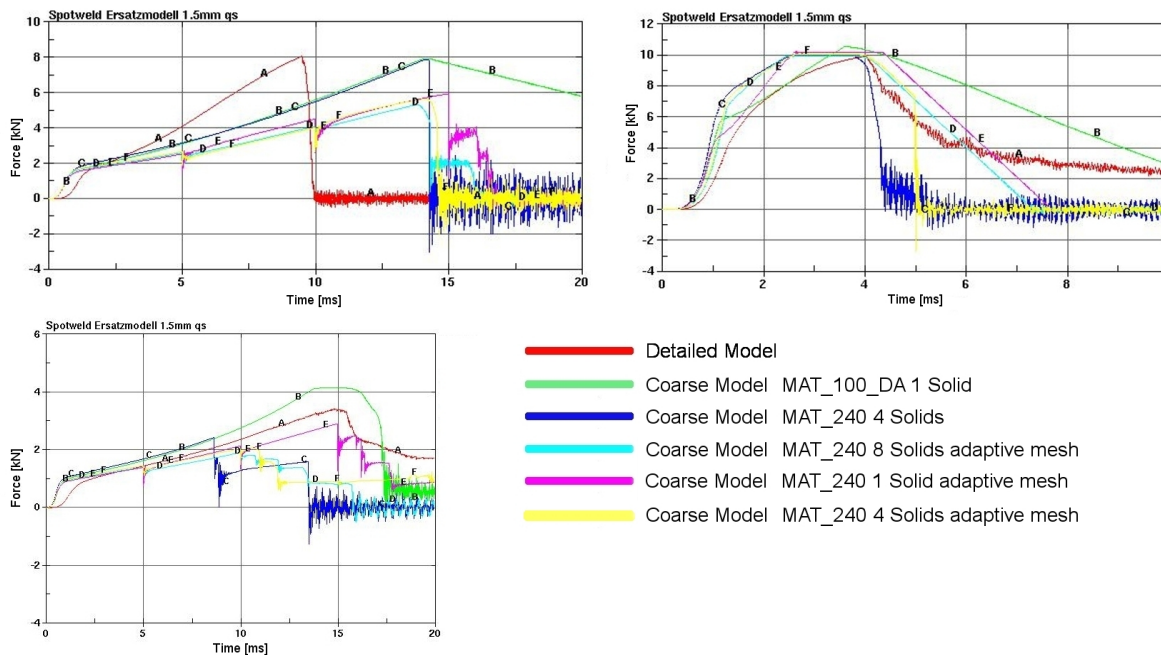


Fig. 16: Tensile (upper-left), shearing (upper-right) and peeling test (lower-left) with an adapted mesh in comparison with the regular mesh.

Changing the spot weld's position by rotating it or the displacement of the mesh shows comparable results as the ones that are already presented above. Again, the change of the spot weld's location has almost no influence on the spot weld's failure behavior during the shearing test simulation, whereas the results for the tensile and peeling tests show that the spot weld's location and its orientation towards the mesh is more important for these load types.

4.4 Influence of the surrounding material

In order to investigate how the sheet metal material grade influences the spot weld's behavior during the computation, the DC04 material parameters were replaced with the stiffer DP600 material parameters. To have a more realistic model, only 16 shell elements surrounding the spot weld were replaced and in a second step, the elements which connected the spot weld directly to the mesh are given the material parameters of the stiffer DP600 sheet metals (Fig. 4). Since the models using four solid elements show the best behavior during the simulations described above, the new models only use four solid elements in combination with *MAT_240.

4.4.1 Replacement of 16 elements around the spot weld with DP600 material parameters

The results above show, that almost the point of failure of the detailed model can be reached with the new model in the tensile test. That seems to be impossible with DC04 material parameters around the

spot weld. The curve's slope during the shearing test simulation is steeper in the beginning but with some adjustments on the *MAT_240 material parameters, the point of failure of the reference simulation can be reached. Compared to the first model, the new model also seems to be closer to the point of failure during the peeling test simulation. Two of the spot weld's solid elements fail before the other two elements. Since the curve for the new model is steeper in the beginning, the force at which the first elements fail is higher. This results in a higher final failure force for the two other elements.

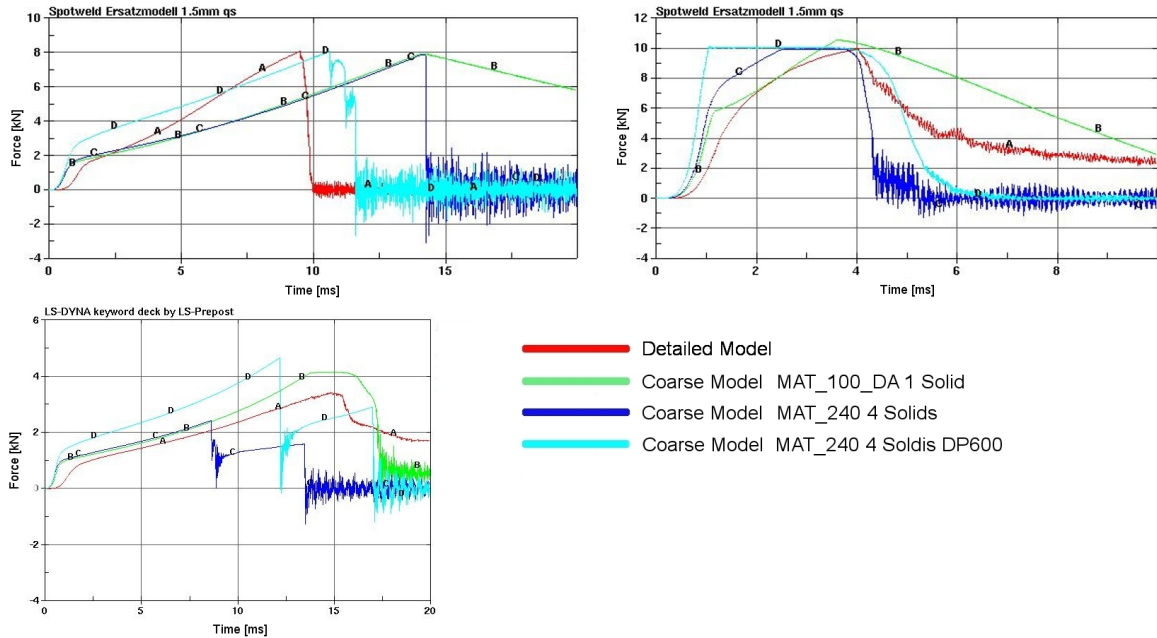


Fig. 17: Tensile (upper-left), shearing (upper-right) and peeling test (lower-left) with DP600 material parameters around the spot weld.

4.4.2 Direct connection between the spot weld and the mesh and replacement of elements surrounding the spot weld with DP600 material parameters

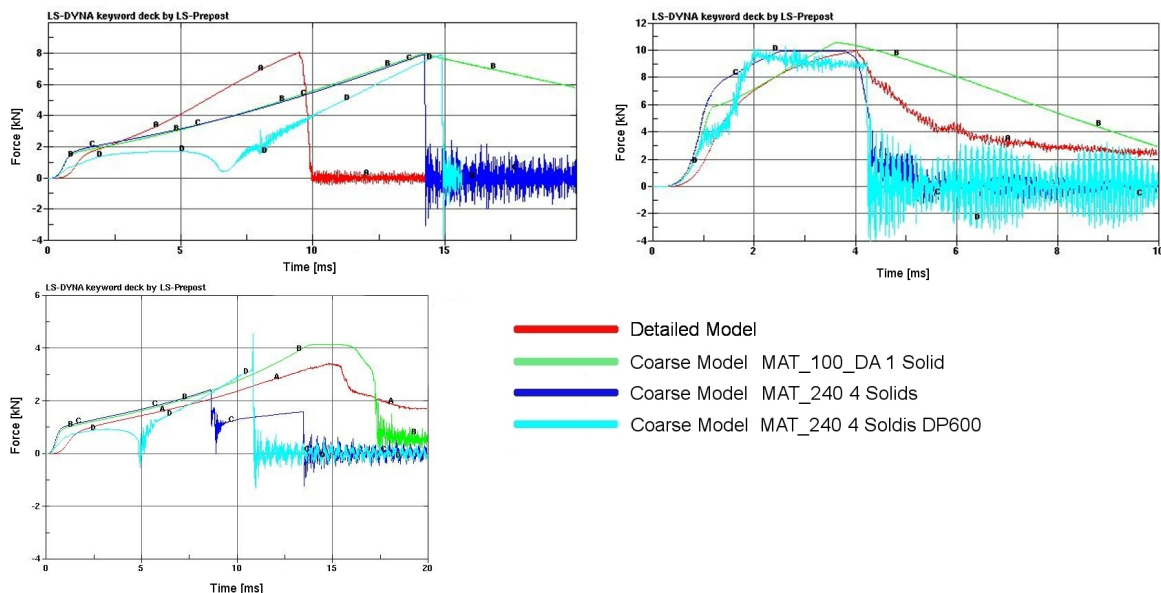


Fig. 18: Direct connecting between spot weld and the mesh – surrounding elements with DP600 material parameters.

A direct connecting between the spot weld and the surrounding sheet metal does not lead to the expected results, even though *MAT_240 material parameters were adapted again. For the tensile

test, at least the point of failure of the coarse *MAT_100_DA model was reached even though there is an unexplained minimum in the force-time (i.e. force-displacement) curve. Nevertheless, the curve for the shear test leads to almost similar results as the curves obtained in all simulations presented above. The only difference can be noted in the fact that the structural answer is very unsteady. The peel test results are not as good as the ones obtained from the computation in (4.4.1).

5 Conclusion

The rate-dependend elasto-plastic material card *MAT_240 was applied for spot weld modeling. Using four solid elements to simulate the spot weld, the spot weld's point of failure was reproduced comparable to another coarsely defined model which uses the *MAT_100_DA material card as the spot weld's material. Especially for the shear test, better results were obtained with *MAT_240.

A displacement of the mesh especially had effects on the spot weld's failure behavior during the tensile and peeling test simulation whereas the model seemed to be stable for shear test simulations. Rotating the spot weld around its z-axis had the same effects on the force-time curves. As we halved the mesh length around the spot weld, we did get good results for a spot weld with the *MAT_240 material and four solid elements – even though the results with the *MAT_100_DA material model and one solid element were the most stable ones. Also the usage of an adaptive mesh and a direct connection between the spot weld and the mesh did not lead to better results.

The usage of one or eight solid elements did not have an influence on the spot weld's point of failure as was expected before the investigation. The beginning of the force-time (i.e force-displacement) curve was almost the same as with four solid elements and therefore, getting any better results as with four solid elements was not expected. Instead, one could show, that the spot weld's failure behavior is highly dependent on the material surrounding the spot weld. When the DC04 sheet metal material was replaced with the stiffer parameters of the DP600 material, one is were able to reproduce the results of the detailed reference model. Using a stiffer sheet metal material resulted in a steeper slope at the beginning of the force-time curve and therefore one could get an earlier failure of the spot weld.

Finally one can conclude that the usage of *MAT_240 as a spot weld material can be beneficial for some load cases: Especially shear loads show a stable answering behavior during the computation. The spot weld behavior is highly dependent on the surrounding material of the sheet metals and therefore it might be worth to change the material configuration close to the spot weld to get the desired, stiffer displacement behavior. Changing the material close to the spot weld may be interpreted as including the effects of heat affected zones and it was possible to get closer to the results of the detailed simulation with less computation time.

6 Literatur

- [1] Livermore Software Technology Corporation: "LS-DYNA Keyword User's Manual, Volume II Material Models", Version 971 / R 5 (Beta), May 2010
- [2] F. Seeger, G. Michel, M. Blanquet: "Investigation on Spot Weld Behavior Using Detailed Modeling Technique", 7. LS-DYNA Anwenderforum, Bamberg 2008, pages B-I-20 – B-I-38
- [3] S. Marzi, O. Hesebeck, M. Brede, F. Kleiner: "A Rate-Dependent, Elasto-Plastic Cohesive Zone Mixed-Mode Model for Crash Analysis of Adhesively Bonded Joints", 7th European LS-DYNA Conference", Salzburg 2009
- [4] Livermore Software Technology Corporation: "LS-DYNA Keyword User's Manual, Volume I", Version 971, May 2007
- [5] Silke Sommer: „Modellierung des Verformungs- und Versagensverhaltens von Punktschweißverbindungen unter monoton ansteigender Belastung“, Band: 2009, 49 Reihe: Schriftenreihe Werkstoffwissenschaft und Werkstofftechnik, 978-3-8322-8519-7, September 2009